

Direct Air-Water Communication with Narrow Beams Laser

As a controlling technique for Guided Surface Torpedoes

Ashraf S. Abdel Halim⁽¹⁾, Mohanad M. Hassan⁽¹⁾

(1) Department of Communication, Faculty of Engineering, Canadian International College (CIC)

Ashraf_Sayed@cic-cairo.com

mohaned_m76459@cic-cairo.com

ABSTRACT

Existing wireless techniques mostly focus on a single physical medium and fall short in achieving high-bandwidth bidirectional communication across the air-water interface. Laser sources enable highly efficient optical communications links due to their ability to be focused into very directive beam profiles. While the scattering in natural waters will cause the beam to broaden, a narrowly directive transmitter can still significantly increase the optical power delivered to a remote under water terminal. We propose a full duplex, direct air-water wireless communication link based on laser beams, capable of adapting to water dynamics with ultrasonic sensing and steering within a full 3D hemisphere using only a MEMS mirror and passive optical elements. In real-world experiments, our system achieves static throughputs up to 5.04 Mbps, zero-BER transmission ranges up to 6.1 m in strong ambient light conditions, and connection time improvements between 47.1% and 29.5% during wave dynamics.

1 Introduction

The underwater world is still largely unexplored, yet surveying and monitoring submerged sites is fundamental for many applications including archaeology, biology and disaster response. It is generally recognized that using multiple heterogeneous cyber physical assets vehicles for a bird's eye view and underwater sensors and vehicles for informed data collection – will advance such efforts. One of the challenges for underwater autonomous deployments is limited communication between assets underwater and in the air. This hinders the situational awareness and coordination of underwater vehicles, data processing, and human supervision. One conventional strategy is to periodically let the underwater vehicle surface to share data, which is inefficient due to time not being spent on the task. Another strategy is to deploy an infrastructure (e.g., network of buoys) at the water surface, connected to both the underwater assets (via acoustic transducers, completely in the water) and the ground station (via tethering or WiFi).

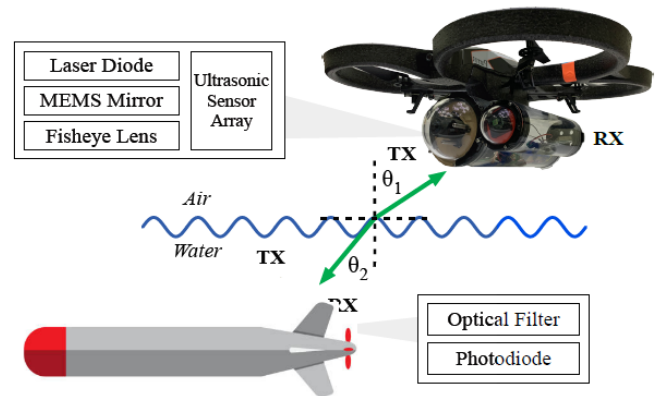


Figure 1: Our envisioned application scenario of air-water communication allowing aerial drones and underwater torpedoes to communicate directly and bi-directionally.

This deployment configuration increases the cost and logistical overhead, limiting the overall scalability. We seek solutions that support direct wireless communication between air and underwater nodes without the need of surface relays. Existing wireless communication technologies, however, mainly focus on a single physical medium and thus do not effectively cross the physical air-water boundary, impairing communication performance. As examples, acoustic communication is the mainstream for underwater scenarios but does not cross the air-water boundary since acoustic waves are mostly reflected by the air-water interface; on the other hand, wireless technologies using radio frequencies (RF) are widely deployed in the air but not underwater since radio signals suffer from severe attenuation in the water (3.5–5 dB/m) and result in short communication ranges. A recent work designs a direct water-air communication link by combining an acoustic link in the water and RF sensing in the air.

Nevertheless, this method only enables a unidirectional link (from water to air), supports only centimeter-level distances above the water, and achieves severely low data rates (400 bps) that are insufficient for most underwater controlling applications.

In this paper, we study the use of laser light to build a high-bandwidth, bidirectional air-water communication link (Fig. 1). Light is the most suitable medium because the majority (90%) of its energy penetrates the air-water interface with only less than 10% energy reflected back.¹ Compared to acoustics, light communication supports much shorter communication latency with faster propagation speeds. Compared to RF, it endures much lower attenuation in the water. In particular, light in the blue/green range (420 nm – 550 nm) attenuates less than 0.5 dB=km in water. We specially consider blue/green laser light because of its superior communication properties: (1) nanosecond-level switching speed, (2) narrow (5–10 nm) spectral power distribution,² allowing optical energy to be concentrated to the wavelength range associated with the smallest attenuation in the water/air, and (3) low beam divergence maximizing the energy efficiency and enhancing communication distance. Gbps level data rates have already been demonstrated using laser light for air-water communication, albeit assuming calm water and with bulky bench-top equipment that are not portable to drones or robots. The key contribution of our work is addressing numerous practical challenges currently unsolved (even with the assumption that the locations of the nodes – one underwater and one in air – are fixed and known) and providing a system framework, Amphi-Light, for a robust laser-based air-water communication link. First, we judiciously design the basic communication link to overcome issues of existing laser hardware and improve its portability for communication. Second, to handle strong ambient light interference, we exploit the narrow spectral power distribution of laser light by placing a narrow optical spectral filter in front of an ultra-sensitive receiver (silicon photomultiplier) to filter out ambient light and maintain sufficient signal-to-noise ratios (including at meter-level distances with low-power laser diodes). Third, to adapt to environmental dynamics, we propose a new optical system to enable precise, full-hemisphere laser steering using low-cost, portable hardware.

It couples a fine-grained MEMS mirror with a miniature fisheye lens to achieve $\sim 90^\circ$ steering range in two dimensions. Finally, we address water dynamics by augmenting the link with ultrasonic sensing and a forecasting method. The ultrasonic sensor array at the transmitter samples the depth of a small number of locations at the air-water interface. These depth values are used to reconstruct a continuous water surface and compute the optimal incident point for the transmitter to steer the laser beam to reach the receiver.

We implement a proof-of-concept Amphi-Light prototype using off-the-shelf hardware. Our prototype consists of the following elements: (1) a self-contained, waterproof laser transmitter utilizing a microcontroller, FPGA, MEMS mirror, and passive optical components; (2) an array of low-cost, ultrasonic depth sensors for reconstructing the water's surface; (3) a waterproof laser receiver capable of detecting the nanosecond laser pulses. We conduct experiments in various settings to examine both link performance and robustness.

We summarize our key findings as below:

- Amphi-Light achieves bidirectional, 5.04 Mbps throughputs with BERs less than 10^{-3} up to 6.5 m in the air and 2.5 m underwater;
- Amphi-Light adapts to wave dynamics (10 – 12 cm wave amplitude and 1-Hz wave frequency) with a 47.1% throughput improvement over no laser steering;
- Amphi-Light is robust against environmental factors including strong sunlight and air/water turbulence at meter ranges;
- The ultrasonic sensing achieves an accuracy of 1.5 cm in the air and 0.5–1.0 cm in the water.

2 System Challenges

Despite the potential of green-blue laser light for direct air-water communication, we face numerous system challenges in achieving high link speed and link reliability. **Laser Hardware Limitations.** Although laser diodes (LDs) are small and relatively inexpensive – making them strong contenders for mobile applications – integrating them into portable platforms for high-speed communication is challenging due to heating and power issues. Our experiments with off-the-shelf LDs show that their temperature rises over time when constantly on.³ The temperature rise causes the central emission wavelength to shift by a few nanometers, which is undesirable as shown later in §3.1. Better heat dissipation requires dedicated temperature controllers and active heat sinks, which are bulky (9 lbs), expensive (~\$1000), and power hungry (up to 60 W).

Additionally, commercial LDs are limited in terms of their optical output powers and wavelength availability. Specifically, blue and green TO-Can LDs are typically limited to 450 nm and 520 nm with optical powers between 30 mW and 140 mW and high power options between 900 mW and 3 W. To maintain stable output power, LDs are typically powered with bench-top power supplies with current and voltage limits or mobile drivers that do not support fast modulation bandwidths (e.g., only up to 2 MHz). The power consumption of low-power LDs ranges from a few m-watts to multiple watts, making mobile-friendly micro-controllers incapable of consistent, safe, and efficient LD operation.

Ambient Light Interference. Given the sparse availability of blue/green LDs, low-power options are the only choice for mobile applications. Thus, strong ambient light, especially in outdoor scenarios, imposes a nontrivial challenge of maintaining high data rates with reasonable signal-to-noise ratios (SNR) at meter-level distances. Even worse, outdoor sunlight can easily saturate sensitive photodiodes (PDs) at the receiver, making it unresponsive to encoded light changes the SNR of an off-the-shelf PD (OPT101) under varying ambient

light intensities. Specially, we collocate a LX1330B light meter with OPT101 and place a 140 mW LD and Osram 5500T03 LED 20 cm away, where the LED light emulates ambient light interference. Next, we vary the intensity of the LED and measure the resulting SNR at the PD. As the LED luminance approaches values associated with outdoor ambient light (e.g., ~10,000 lx in indirect sunlight), the SNR quickly drops below 3 dB (specially, 3.2 dB at 5700 lx and 0.6 dB at 8070 lx). Furthermore, PDs capable of detecting low-level light need to have sufficiently high gain, making them susceptible to saturation under intense ambient light (the OPT101 became saturated when the LED intensity approached 14,500 lx).

Laser Beam Steering. Supporting arbitrary underwater/ torpedo locations demands precise steering of the narrow laser beam in a wide range. Existing laser steering mechanisms, however, face a fundamental trade off between steering range and granularity. Traditionally, FSO beam steering uses mechanical gimbals for 360° coarse-grained steering and then additional mechanisms for secondary, fine-grained adjustments. Although mechanical gimbals can support a large angular steering range, they are bulky, imprecise, and not intended for use in mobile settings. On the other hand, the mechanisms used for fine-grained steering (e.g., micro electromechanical-systems (MEMS) mirrors, acousto-optic detectors (AODs), tunable lenses) only achieve millirad/single degree steering ranges [constraining the receiver location to a narrow cone around the transmitter]. Environmental Dynamics. In real world environments, such as lakes or oceans, the water's surface is dynamic, rendering a laser link unsustainable due to refraction at the air-water interface. The impact of water dynamics is twofold:

(1) A change in water level caused by precipitation or a tide can disrupt the optical link permanently. For example, a rise in the water level will move the incident point on the surface to a new position if the incident angle is not 0°. Consequently, the refracted light will be translated and miss the underwater receiver (Fig. 2(a)). Based on geometry, the horizontal displacement of the light beam is $\Delta h(\tan\alpha \tan\beta)$, where Δh is the level change, α is the incident angle, and β is the angle of refraction. A level change of 1m4 with a 30° incident angle results in 17 cm displacement of the beam, far beyond the diameter of common light sensors (a few mm); (2) Periodic surface waves caused by wind or moving objects can swing the refracted light around the receiver. The oscillation causes the optical link to deviate from the receiver (Fig. 2(b)). Our experiment shows that waves with ~10 cm peak-to-peak amplitudes make the link unavailable for ~70% of the time.

1 Basic Laser Link Design

We present the basic laser communication link design able to (1) achieve sufficient data rates (i.e., Mbps for underwater drone communication and sensing) with off-the-shelf laser diodes and (2) support a hemispherical steering range to connect the transmitter and receiver at arbitrary locations.

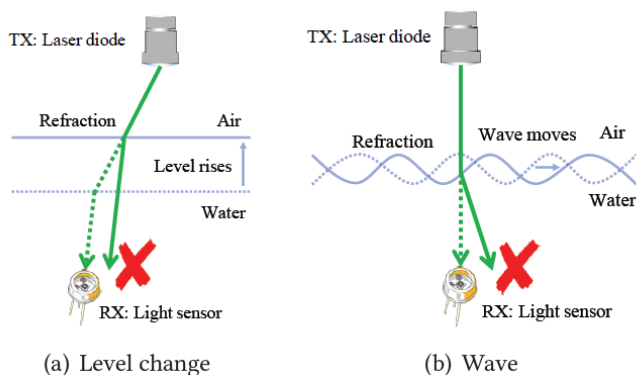


Figure 2: Water dynamics degrade the link reliability due to light refraction at the air-water interface. (a) Precipitation and tide can raise the water level, which permanently translates the refracted light and disrupts the aligned link. (b) Periodic waves can swing the refracted light, resulting in recurrent misalignment with the receiver.

3.1 Transmitter & Receiver

Transmitter. To support Mbps throughputs and low energy consumption – important tradeoff_ design for underwater drones – we adopt the DarkLight concept in [65]. Specifically, DarkLight applies overlapping pulse position modulation (OPPM), where data is encoded into the position of the rising edge of a light pulse within a symbol. We extend DarkLight to LDs, leveraging LD’s fast switching speeds to increase the data rate while still maintaining a low duty cycle. This leads to a significant improvement in throughput from Kbps with LEDs to Mbps with LDs, as shown later in §6. Reducing the duty cycle removes the need for a dedicated temperature controller as the laser will remain o_ the majority of the time. Furthermore, a low duty cycle reduces the power consumption issues typically associated with laser communication, allowing us to power the LD with a microcontroller without sacrificing the data rate. Even though OPPM is the most suitable choice for sustained communication5 given the current laser hardware limitations, the AmphiLight framework is general and can be combined with other modulation schemes. As advances in LD hardware will better address heating6 and power issues in the future, other modulations schemes such as OOK or OFDM can be easily integrated into AmphiLight to further boost link data rates. However, with higher-power modulation schemes, the effects of turbulence, especially over long distances, might degrade the overall link quality. Regardless, fully leveraging the GHz switching speeds of LDs, an OOK implementation could achieve throughputs in the Gbps range with only a few mJ/bit. Receiver. We address the key challenge of the receiver design – to extract signals from low-power LDs amid strong ambient light interference while maintaining meter-level distances – via two design elements. First, we add a narrow optical band pass filter (\$30 – \$200) that allows only the narrow wavelength range of the laser light (confined only to a few nm [53]) to pass, and filter out the majority of the ambient light energy and significantly boost the signal-to-noise ratios (SNRs). As an example, Fig. 3 plots the spectral power distribution of outdoor sunlight (measured on a sunny noon in August, 2019), as well as that of a low-power LD [13], measured by a Thorlabs CCS100 spectrometer.

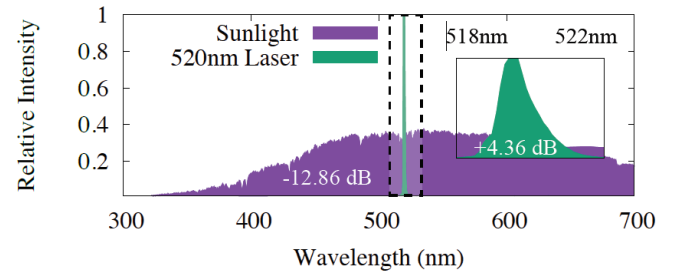


Figure 3: The relative intensity spectrum of the sun compared to a low-power LD. Utilizing a narrow band pass filter from 518 nm to 522 nm, the SNR can be increased from -12.86 dB to 4.36 dB.

We observe that the weak laser light is buried in the strong sunlight. Nevertheless, adding an o_-the-shelf band pass filter [12] with a -or+2 nm bandwidth, we drastically improve the SNR. Additionally, spectral filtering also addresses the problem of sensor saturation under strong ambient light. Second, we utilize an ultra-sensitive silicon photomultiplier (SiPM) light sensor, i.e., an array of avalanche photodiodes (APDs), with high gains, large active areas, and large angular responses [14].7 Given the SiPM’s significantly higher gain compared to traditional light sensors, we are able to maintain a sufficiently high SNR even with low-powered LDs at meter-level distances. We further increase the SNR by using an RF amplifier with a DC-bias cutoff allowing us to amplify only the low-power laser light.

3.2 Full-Hemisphere Beam Steering

We adapt the fine grained steering mechanism from FSO by expanding its limited steering range with a judiciously designed optical circuit. Specially, we combine a small angle MEMS mirror with a miniature fisheye lens [24] to enlarge the small-angle steering to – or +90° in two dimensions. As shown in Figure 4(a), a fisheye lens is a combination of wide-angle lenses typically used to create hemispherical images for photographs. Fisheye lenses concentrate light rays coming from a full hemisphere to a small image plane at the focal length, limited by the form factor of digital camera image sensors.

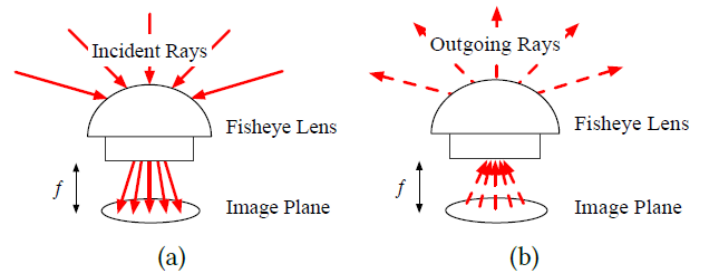


Figure 4: (a) Light enters the fisheye lens and is projected onto a small image plane, compressing the wide incoming light directions into a smaller range. (b) We consider the inverse of the propagation path to enlarge a narrow steering range to full hemisphere.

We exploit this optical feature to expand the narrow steering range of MEMS mirror. Specially, given the path symmetry of light propagation, we consider the inverse direction of the light path by sending a light ray through the image plane. This leads to an outgoing light ray steered to a larger irradiance angle (Fig. 4(b)), thus expanding the small input steering range to an entire hemisphere. Fig. 5 shows the optical circuit for laser beam steering. An achromatic triplet lens [83] is added to keep a constant focal point on the fisheye lens (i.e., correcting for spherical aberrations) [15]. It also concentrates the outgoing light ray from the MEMS mirror to the image plane of fisheye lens to match the desired inverse propagation path.

4 Addressing Water Surface Dynamics

Armed with the basic link design, we now set out to address challenges from dynamics at the air-water interface, aiming to improve link robustness in practical settings. To mitigate the misalignment caused by water dynamics, a straw-man approach is to expand/diffuse the laser beam to keep the receiver within the light coverage during water dynamics. This approach, however, greatly lowers the energy efficiency of communication and demands high-power LDs to support meter-level distances. Another approach is to blindly steer the laser beam and scan all directions to search for the direction that reaches the receiver. The resulting overhead to scan the whole steering range (up to hundreds of ms with existing MEMS mirrors), however, reduces the link throughput. It also requires a feedback channel from the receiver, which may be equally unavailable due to misalignment.

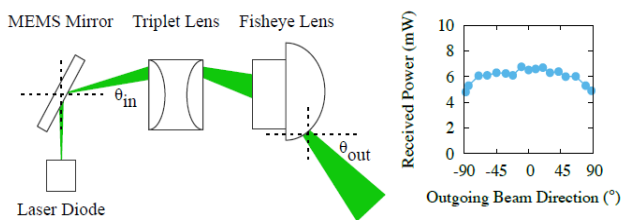


Figure 5: Our proposed optical circuit design, using a small-angle MEMS mirror and fisheye lens. Not only can we achieve a full $-$ or $+90^\circ$ range in two dimensions, but the received power only deviates by 28% at extreme angles.

Instead, we consider a more proactive approach where the system continuously senses the condition (both the water level and the shape of the wavy surface) of the air-water interface, computes the optimal direction to reach the receiver, and then steers the laser beam correspondingly to sustain the link's connection (Fig. 6).

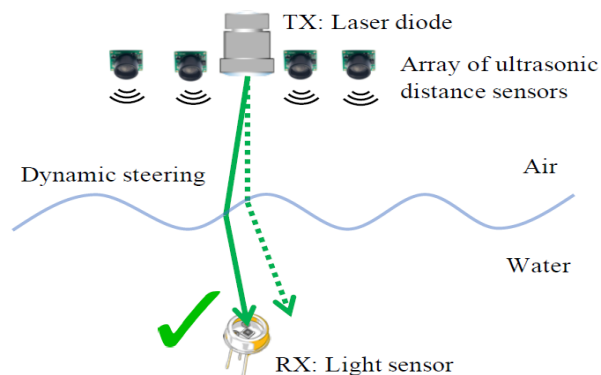


Figure 6: Addressing water dynamics by continuously sensing the water with an array of ultrasonic sensors, interpolating the surface, computing the optimal path to the receiver, and steering the laser.

4.1 Sensing Waves

To sense the water surface condition, we start by examining the efficacy of existing techniques. Vision-based methods with depth cameras have been widely used to reconstruct the 3D shape of objects. These methods, however, are unable to sense the shape of water surfaces because light mostly penetrates the air-water interface and reflects almost no light for the depth camera to reconstruct the surface. Our experiments with an Intel Real Sense D435i depth camera shows that depth information is only correct when a piece of paper is placed on the water surface. Alternatively, one can consider RF-based methods, i.e., mmWave radar which has been shown to sense the distance from air to water at μm -level accuracy [67]. Given the severe attenuation of RF signals in the water, however, RF-based methods cannot be applied to underwater transmitters for sensing the water surface. Additionally, reconstructing the water surface requires an array of mmWave radars that can cost thousands of dollars. The above exploration leads us to consider the acoustic medium. Specially, we consider ultrasonic distance sensors to avoid interference from ambient noises. Ultrasonic distance sensors work in both air and water, and thus can be used by both aerial and underwater transmitters to sense the air-water interface and adapt the outgoing laser beam direction. Additionally, the accuracy of ultrasonic distance sensors are on the mm-level and are affordable (e.g., \$1 each). Depth Sampling via Ultrasonic Sensing. To sense the shape of the water surface, a single ultrasonic sensor is insufficient. Instead, we employ an array of M sensors that are uniformly distributed on the transmitter plane. Because all sensors operate at the same acoustic frequency and are close to each other, simultaneous measurements cause interference. Therefore, we instruct the sensors to sample the distance sequentially.

The sequential measurements result in a sensing latency that grows linearly with the number of sensors and proportionally to the distance between the transducers and water surface. In our implementation with 16 sensors, generating each snapshot of the surface is approximately 50 ms (20 Hz frame rate) which can impair the efficacy of beam steering for faster waves. To lower the latency of the sensor array, we propose to forecast the height samples of the water surface. Instead of waiting for the readings from all sensors to be ready, we can forecast the distances based on historical data. It is possible to forecast the height of the water because water surface waves are periodic. Specially, we output distances from all sensor positions once a new reading is available from a sensor (e.g., at time t_{cur}). If the readings from other sensors are not ready at that time, we will use the forecasted distances. Because the water wave is periodic, we can use the Fourier transform for forecasting, i.e., estimate the frequency and phase of the waves despite the variable latency. Specially, we buffer a window of the most recent N readings for each sensor x_k ($k \in [0, N-1]$) compute the Discrete-time Fourier Transform (DFT) in the window, estimate the period of the major frequency component T , and forecast the reading x_N by linear interpolation at time x_{N-T} . If the timestamp of x_N is ahead of t_{cur} , we will linearly interpolate between x_{N-1} and x_N . Our measurements show that the forecast distances using historical readings align well with the measured distances. Forecasting reduces the sensing latency of each frame (i.e., time period between adjacent frames) to 1/16 of the non forecast method, approximately 3 ms. Since the movement of the water waves between frames is the source of sensing errors, the forecasting error is 1/16 of the non-forecast error.

This forecasting method assumes a single major frequency in the water waves. For more complicated waves, in the future we can investigate advanced forecasting methods, such as ARIMA and RNN (which require training and higher computational cost).

Reconstructing Wave Surface. To reconstruct a continuous wave surface for every frame, we need to interpolate between the discrete distance samples output by the array. We adopt a bicubic surface model to fit the outputs:

$$h(x, y) = \sum_{i=0}^3 \sum_{j=0}^3 a_{ij} x^i y^j,$$

where (x, y) is the coordinate on the horizontal plane relative to the center of the sensor array, $h(x, y)$ is the height of wave at (x, y) , and a_{ij} 's are the parameters of the surface. Bicu bic surface is widely used in 2D interpolation. We choose this model for its shape flexibility and computational simplicity. We use the model using linear regression, which is computationally inexpensive and suitable for real-time reconstruction. The linear system is $\mathbf{h} = \mathbf{X} \boldsymbol{\beta} + \beta_0$, where \mathbf{h} is a vector of the measurement distances by each sensor, and \mathbf{X} is a matrix that is constructed by the coordinates of the sensors. Put formally, \mathbf{X} is calculated as:

$$\mathbf{X} = \begin{bmatrix} x_1^3 y_1^3 & x_1^3 y_1^2 & x_1^3 y_1 & x_1^3 & \cdots & y_1^3 & y_1^2 & y_1 \\ x_2^3 y_2^3 & x_2^3 y_2^2 & x_2^3 y_2 & x_2^3 & \cdots & y_2^3 & y_2^2 & y_2 \\ \vdots & \vdots & \vdots & \vdots & \ddots & \vdots & \vdots & \vdots \\ x_M^3 y_M^3 & x_M^3 y_M^2 & x_M^3 y_M & x_M^3 & \cdots & y_M^3 & y_M^2 & y_M \end{bmatrix}$$

where each row is for a sensor. The coefficients $\boldsymbol{\beta}$ and β_0 are the parameters of the surface, i.e., $\boldsymbol{\beta} = \{a_{ij} | i, j \in \{0, 1, 2, 3\}\} - \{a_{00}\}$. The model, therefore, contains 16 parameters in total. With M ultrasonic sensors and thus M measurements, we employ regularized linear regression to prevent over fitting and the loss function

$$f(\boldsymbol{\beta}, \beta_0) = \sum_{i=1}^M \left(h_i - \beta_0 - \sum_{j=1}^{15} \beta_j X_{ij} \right)^2 + \lambda \sum_{j=1}^{15} \beta_j^2,$$

is : where λ is a hyper-parameter that controls the penalty on the parameters. In our implementation, $\lambda = 5 \times 10^{-5}$.

4.2 Computing the Incident Point

Once the shape of the surface wave is estimated, we next seek an incident point on the surface such that the refracted light can reach the receiver. The incident light and refracted light must be subject to Snell's law. However, this equation is intractable because of the trigonometric functions, i.e, we have to solve the incident point position numerically. First, we model the problem as an optimization problem (Fig. 7).

For every possible point on the surface, we are able to determine the direction of the refracted light (\vec{r}) according to Snell's law and the direction from the incident point to the receiver (\vec{t}). If the discrepancy between the two directions (θ) is zero, the previous equation is exactly solved. Therefore, we are looking for the incident point that minimizes the discrepancy θ , i.e., maximize $\cos \theta$:

$$\text{Maximize} \quad \cos \theta = \frac{\vec{r} \cdot \vec{t}}{|\vec{r}| |\vec{t}|} \quad (1a)$$

$$\text{subj. to:} \quad \vec{r} = p \vec{m} + \vec{n} \quad (1b)$$

$$p = \frac{p |\vec{m}|}{|\vec{n}|} = \frac{\sin \beta}{\sin(\alpha - \beta)} \quad (1c)$$

$$\vec{n} = \left(\frac{\partial h}{\partial x}, \frac{\partial h}{\partial y}, -1 \right) \quad (1d)$$

Here \vec{n} is the surface normal unit vector, \vec{m} is the direction vector of the incident light, n_{water} is the refractive index of water, and $\frac{\sin \alpha}{\sin \beta} = n_{\text{water}}$. To calculate \vec{r} , we first determine the direction of the surface normal \vec{n} according to 1d. Suppose the direction vector of the incident light is \vec{m} , which

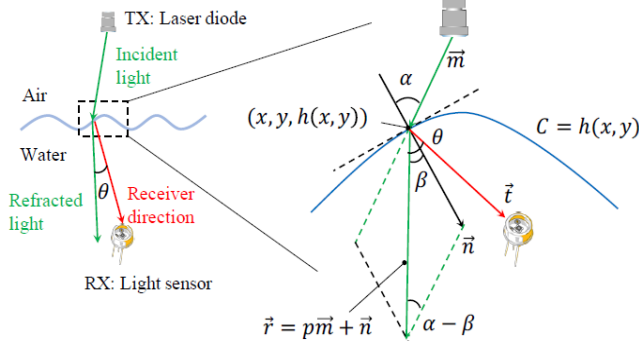


Figure 7: Geometric model of finding the optimal path to reach the receiver. We model finding the incident point on the surface such that the laser can reach the receiver as an optimization problem. This figure shows a single solution in the solution space, where the optimization happens over all possible solutions. We minimize the angle discrepancy (q) between the refracted light (\vec{r}) and the target path that reaches the receiver (\vec{t}) subject to Snell's law which governs the relation between the angles of incidence (a) and refraction (b).

is also a unit vector. According to Snell's law, the incident light, the refracted light, and the surface normal are coplanar. The refracted light's direction can thus be written in the form of 1b, where p is calculated according to law of sines and Snell's law (1c). Assuming the transmitter is in the air and the receiver is underwater, n_{water} is the refractive index of water (we can take the reciprocal if the transmitter and receiver exchange positions). Notice that all the quantities are functions of (x, y) .

Algorithm 1: Find outgoing beam direction

```

Input:  $p_0$ : initial incident point,  $r$ : receiver position,  $b$ : surface
      shape parameters // TX: (0,0,0)
Output:  $(\gamma_x, \gamma_y)$ : outgoing beam angle along x-axis and y-axis
 $\alpha \leftarrow 0.01$  // learning rate
 $p_n \leftarrow p_0$  // next point to test
 $\epsilon \leftarrow 0.005$  // accuracy tolerance
 $N \leftarrow 100$  // max iteration
for  $i \leftarrow 1$  to  $N$  do
     $p \leftarrow p_n$ 
    /* compute gradient and error */
     $\nabla_x e \leftarrow \text{gradient}(p, r, b)$ 
    if  $e < \epsilon$  then
        break
     $p_n = p + \alpha \nabla$ 
end
 $z = h(p)$  // z coordinate on surface
 $\gamma_x = \arctan(p_x / \text{abs}(z))$ 
 $\gamma_y = \arctan(p_y / \text{abs}(z))$ 
return  $(\gamma_x, \gamma_y)$ 

```

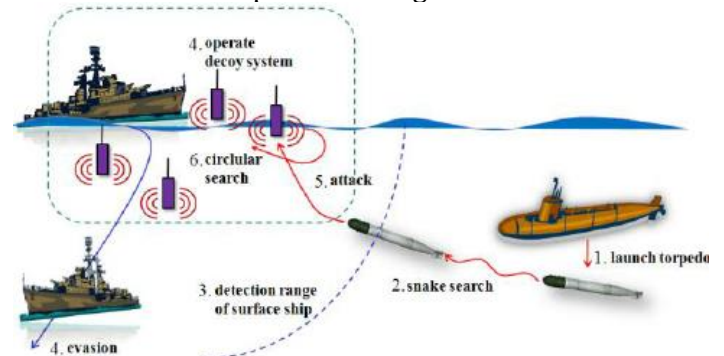
We solve the optimization problem by gradient ascent (Algo. 1). We compute the gradient ($\nabla \cos \theta$) following the chain rule. For each frame, we set the initial incident point as the incident point of the previous frame. The spatial and temporal continuity of the water wave and the observation of the optimization result show that the new incident point should be close to the previous one because the change of the surface shape is small between adjacent frames. All the computation, including the forecasting, surface reconstruction, and path finding, can be completed within 1 ms. Note that wave sensing, path finding, and beam steering occur in parallel with the data transmission, incurring no overhead on the optical link. Notably, our algorithm has the potential to fail if some of the characteristics are beyond the sensing capabilities of the ultrasonic array: wavelength is smaller than the separation between the ultrasonic sensors; wave frequency is higher than the sensing frequency.

4.3 Related military applications

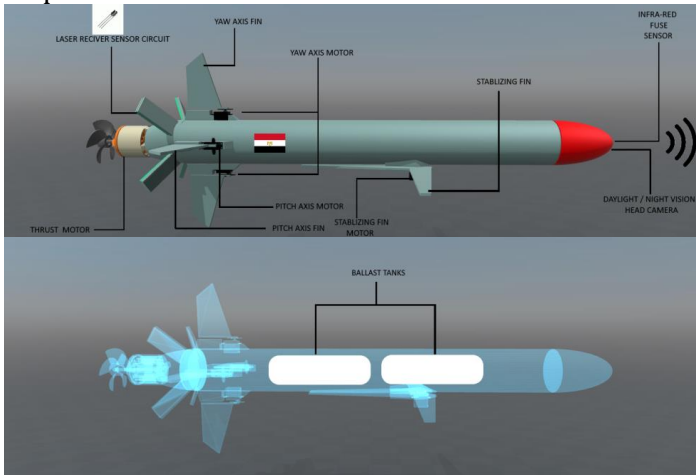
Torpedoes are the most preferred lethal underwater weapons for naval platforms such as submarines, surface vessels, aircraft and helicopters. Naval-technology.com lists the world's most advanced torpedoes based on performance characteristics such as speed, range and operating depth.

We could use the narrow beam optical under communication system as a controlling system for medium or long-range electrical Guided Torpedo. This new technique can make this type of Torpedo to be more effective more than ordinary torpedo which Its main concept depends on acquisition waves propagation as a technique to drive the torpedo automatically as shown in following figure ,

This old technique can be overcome by naval maneuvers and anti torpedoes systems or simply any object will pass through the torpedo path may disturb It and make the torpedo to change Its course .



Applying This makes the torpedo harder to be tricked Because Its remotely controlled by human who homes the torpedo to the desired target . As a result It does not affected by anti-torpedoes , In addition to being Agile Due to Its battery bank Which allow them to move for very large distances With an excellent Speed to follow and track the target . This Torpedo controlling system rely on laser optics narrow beam as a channel for the communications link between the fired-by ship and the torpedo .



Conclusion

We presented a new system framework that enables full duplex air-water communication link using narrow beam laser light. Final results showed throughputs up to 5.04 Mbps at 6.5 m in the air and 2.5 m underwater, making this technique a promising technology to be deployed on under water systems that require a full duplex communication link , making It excellent approach to apply for guided torpedoes systems .

References

- [1] Bandpass filter tutorial. https://www.thorlabs.com/newgrouppage9.cfm?objectgroup_id=10772.
 - [2] Cree XLamp CXA2520 LED. <https://www.cree.com/led-components/media/documents/ds-CXA2520.pdf>.
 - [3] Daylight. <https://en.wikipedia.org/wiki/Daylight>.
 - [4] Dispersion. [https://en.wikipedia.org/wiki/Dispersion_\(water_waves\)](https://en.wikipedia.org/wiki/Dispersion_(water_waves)).
 - [5] Electromagnetic absorption by water. https://en.wikipedia.org/wiki/Electromagnetic_absorption_by_water.
 - [6] Hc-sr04 ultrasonic sensor distance module. https://www.amazon.com/gp/product/B07H5D43QH/ref=ppx_yo_dt_b_asin_title_o04_s00?ie=UTF8&psc=1.
 - [7] Laser diodes. https://www.rp-photonics.com/laser_diodes.html.
 - [8] Ted200c operation manual. <https://www.thorlabs.com/thorproduct.cfm?partnumber=TED200C>.
 - [9] Visible laser diodes: Center wavelengths from 404 nm to 690 nm. https://www.thorlabs.com/newgrouppage9.cfm?objectgroup_id=7.
 - [10] Waterproof ultrasonic module jsn-sr04t. https://www.alibaba.com/product-detail/Waterproof-Ultrasonic-Module-JSNSR04T-Water_60609536665.html?spm=a2700.wholesale.maylikeexp.1.33b22332i9KFmB.
- <https://courses.physics.illinois.edu/ece598hh/fa2020/papers/carver.pdf>